16th ICAAR
LISBOA 2020-2022

16th International Conference on
Alkali-Aggregate Reaction in Concrete
Lisboa | LNEC | Portugal | 31 May - 2 June 2022
http://icaar2020-2022.lnec.pt

Influence of the direction on alkali-aggregate reaction (ASR)-induced distress of reinforced concrete members

Gabriella Andrade [(1)], Agnes Bezerra [(2)], Leandro Sanchez [(3)], Benoit Fournier [(4)]

(1) University of Ottawa, Ottawa, Canada, gandr070@uottawa.ca

(2) University of Ottawa, Ottawa, Canada, abeze037@uottawa.ca

(3) University of Ottawa, Ottawa, Canada. leandro.sanchez@outtawa.ca

(4) Laval University, Quebec, Canada. benoit.fournier@ggl.ulaval.ca

Abstract

Robert-Bourassa/Charest (RBC) overpass (Quebec, Canada) was a concrete structure severely affected by alkali-silica reaction (ASR) due to the use of a highly reactive coarse aggregate (local siliceous limestone) in the concrete construction. Over the years, RBC overpass was monitored, and several laboratory test procedures were conducted on cores extracted from the different members of the structure. RBC was finally demolished in 2010-2011 and thus, two 3-meter sections of the reinforced columns, one coming from an exposed site and the other from a non-exposed location (i.e. under the bridge deck) were gathered and stored in the laboratory for further analyses. This paper presents the results of the multi-level assessment (i.e. microscopic and mechanical) performed on cores extracted from distinct directions (i.e. vertical, longitudinal and transverse) from the exposed and non-exposed RBC columns. Furthermore, the appraisal of the stirrups stress-state on the reinforced members was also performed. Results show that ASR-induced damage varies according to the columns exposure conditions and coring direction.

Keywords: alkali-aggregate reaction; structural implications; aging infrastructure; concrete structures

1.   INTRODUCTION

Robert-Bourassa/Charest (RBC) was a highway overpass built in 1966 using an alkali-silica reactive limestone aggregate (dark-grey, fine-grained Ordovician limestone). The structure was made of a deck resting on reinforced concrete Y-shaped columns, themselves supported by massive concrete foundations (Figure 1.1). Technical reports indicate that the 28-day concrete design strengths were 24 MPa for the foundation blocks and 28 MPa for the columns and decks; however, no specific information is available on the concrete mix-designs used for construction [1].

Figure 1.1: Robert Bourassa/Charest overpass

The structure has developed many signs of distress over the last 30 years on the various elements (deck, foundation, columns), such as steel corrosion and concrete delamination/spalling at the level of the deck; map cracking, scaling, disaggregation and pop-outs affecting the foundations due to ASR and freeze-thaw (FT) cycles; as well as concrete spalling and steel corrosion on the columns and foundations exposed to de-icing salt-water sprayed from traffic on the Robert-Bourassa highway [2]. Several inspections and laboratory tests were performed on the RBC bridge and cores extracted from its different structural elements. Considering the investigations executed on the bridge, Bérubé et al. developed a guide for the diagnosis, prognosis and management of AAR-affected structures using a number of laboratory tests (such as the Damage Rating Index (DRI), Stiffness Damage Test (SDT), residual expansion, water soluble alkali, etc.) to assess the degree of deterioration of affected concrete members as well as their potential for further induced damage [3].

RBC overpass was demolished in 2010/2011, yet prior to the demolition, two 3-meter sections of the reinforced columns were sawed and brought to the laboratory for further analyses; one coming from an exposed site and the other from a non-exposed location. Then, several cores were drilled along the three main directions (i.e. longitudinal, vertical and traversal) from each column. Thus, the condition assessment of the columns was performed through the use of a multi-level assessment as proposed by Sanchez et al [4-8]. Furthermore, the stress-state of the stirrups was appraised by removing the concrete cover at designated locations, installing strain-gauges on the stirrups, cutting them and measuring their stress-relief. The latter was conducted to verify whether ASR might have contributed to the yielding of some stirrups as previously reported in Japan [9].

2. SCOPE OF THE WORK

RBC demolition took place in 2010-2011 and represented an immense opportunity to further study and understand distinct parameters influencing on ASR-induced expansion and damage in real concrete structures. This paper presents a thorough assessment of two 3-meter sections of RBC columns from exposed and non-exposed locations with the aim of understanding the influence of the direction (and confinement effects) on ASR-induced distress of reinforced concrete members. Cores were extracted from distinct directions (i.e. vertical, longitudinal and transverse) from the exposed and non-exposed columns and condition was assessed through the multi-level assessment as per Sanchez et al. [4-8]. Furthermore, the stress-state of the stirrups were appraised to check the likelihood of their yielding after 50 years of service.

3. MATERIAL PROPERTIES

Cores were drilled along the three main directions longitudinal, vertical and transversal (identified as L, V and T in this work) from two 3-meter sections of RBC reinforced columns (one coming from an exposed site (E) and the other from a non-exposed location (NE)), both illustrated in Figure 3.1. Once extracted, all cores were saw cut to have 100 by 200 mm in size, wrapped in plastic film and stored at 12°C to stop further ASR development.

| (a) | (b) |

Figure 3.1: (a) Non-exposed column, (b) Exposed column

Prior to mechanical testing, the ends of the cores were mechanically ground so that flat surfaces might have been achieved. The samples were also re-conditioned through 48 h in the moist curing chamber as proposed by Sanchez et al [6]. The specimens selected for microscopic analysis were cut in two, axially, and one of the flat surfaces was polished using a standard polishing device which uses diamond-impregnated rubber disks (No 50 [coarse], 100, 400, 800, 1500, 3000 [very fine]); this device was found

most suitable for the work, as it does not loose abrasive powders that can fill up cracks or voids in concrete, and high quality polishing is obtained with minimal water supply so that AAR-gel leaching is avoided. Afterwards, the DRI was performed as per Sanchez et al. [7]. It is worth mentioning that due to the severity of its deterioration, the E column has been wrapped with Fibre Reinforced Plastic (FRP) sheets back in 2000, while the NE column had only been treated with a waterproof compound.

3.1 Microscopic Procedures

3.1.1 Damage Rate Index

The Damage Rating Index (DRI) is a widely used semi-quantitative petrographic technique proposed by Grattan-Bellew and Danay to evaluate the damage degree of AAR affected concrete [10-12]. It consists of an evaluation of affected polished concrete sections under a stereomicroscope with 15-16x magnification, where distinct damage features associated with AAR are quantified through 1 cm^2 grids drawn on the polished samples. The damage features are then multiplied by weighing factors whose purpose is to balance their relative importance. At the end of the analysis, a DRI number is calculated; the higher the number, the higher AAR-induced damage. Over time, researchers improved the procedure to better represent "damage" in its broader sense, while reducing its subjectivity and variability amongst operators [12]. They suggested the same weighing factors to be used for open cracks within the aggregates with or without reaction products (i.e. gel) along with cracks in cement paste with or without reaction products (Table 3.1).

In this work, samples from E and NE columns were cored, polished and evaluated from distinct directions (i.e. vertical, longitudinal and transverse) through the DRI as per the recent version proposed by Sanchez et al. [11].

Table 3.1: Weighing factors for petrographic features classification [11]

Petrographic features		Weighting factors
Crack in coarse aggregate	CCA	0.25
Opened crack in coarse aggregate	OCA	2
Crack with reaction product in coarse aggregate	OCAG	2
Coarse aggregate de-bonded	CAD	3
Crack in cement paste	CCP	3
Crack with reaction product in cement paste	CCPG	3
Air void lined / filled with gel	AVG	--
Reaction rim around aggregate	RR	--
Disaggregate / corroded aggregate particle	DAP	2

Some of those features can be seen Figure 3.2, such as open cracks in the aggregate (OCA), closed cracks in the aggregate (CCA), open cracks in the aggregate with gel (OCAG), and cracks in the cement paste with gel (CCPG).
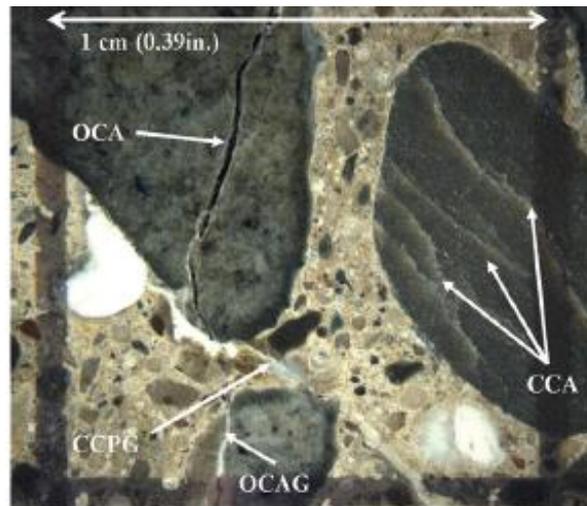
Figure 3.2: Petrographic features of different cracks [11]

3.1.2 Crack pattern

Assessment through the use of image analysis was also conducted on the cracks amount and pattern from exposed versus non-exposed columns. Therefore, one of the columns ends was polished using a portable hand-polishing machine as per the same procedure conducted for DRI analysis. Then, high quality pictures were taken, and the *ArcGIS* software was selected to highlight macrocracks (i.e. red traces) and microcracks (i.e. blue traces). In this work, macrocracks have been classified as cracks with openings greater than 0.3 mm.

3.2 Mechanical Testing

3.2.1 Stiffness Damage Test (SDT)

The *Stiffness Damage Test* (SDT) was performed to quantify the damage degree of concrete affected by AAR [4-7]. The method is based on a cyclic loading (using 40% of the compressive strength of "sound" concrete of similar characteristics/mix design) of concrete samples (cylinders or cores). The full procedure is described in Sanchez et al. [4-6] and the same parameters were adopted in this study. Using a controlled loading rate of 0.10 MPa/s, five cycles of loading/unloading were applied on each set of samples. Each set is comprised of four to six concrete cores extracted from the same column section and direction (i.e. E vs. NE; longitudinal, transverse, and vertical).

3.3 Stress-state of the stirrups

Besides the above microscopic and mechanical assessments, evaluations were also performed on the stress-state of the stirrups of both columns (NE & E). Therefore, at designated locations, the concrete cover was removed, and the stirrups sanded and cleaned. Then, strain-gauges were glued on the stirrups in order to measure their stress relief upon cutting. Six stirrups were selected for testing at each column.

4. RESULTS

4.1 Damage Rate Index (DRI)

Figure 4.1 gives a plot of the DRI numbers as a function of the exposure and direction of the cores studied in this work. First of all, it is possible to observe that all samples presented some closed cracks within the aggregate particles (CCA - blue charts). This petrographic feature is not necessarily related to ASR development but rather with the aggregate's crushing and or weathering processes. However, all the cores evaluated in this work presented important amounts of open cracks with or without gel within the aggregates (OCA and OCAG - red and green charts, respectively) along with cracks in the cement paste with and without gel (CCP and CCPG – orange and dark blue charts). All these features clearly indicate the presence of ASR deterioration.

Analyzing Figure 4.1, one verifies that the DRI numbers from the exposed columns roughly varied from 720 to 942, whereas from 506 to 566 for non-exposed columns. The latter seems to indicate that the exposure conditions indeed influence ASR-induced development, as expected. Furthermore, distinct DRI results were also found as a function of the cores direction. For both columns, the transverse cores yielded higher damaged (i.e. DRI numbers), followed the vertical and longitudinal cores. These results were more evident for the exposed columns.
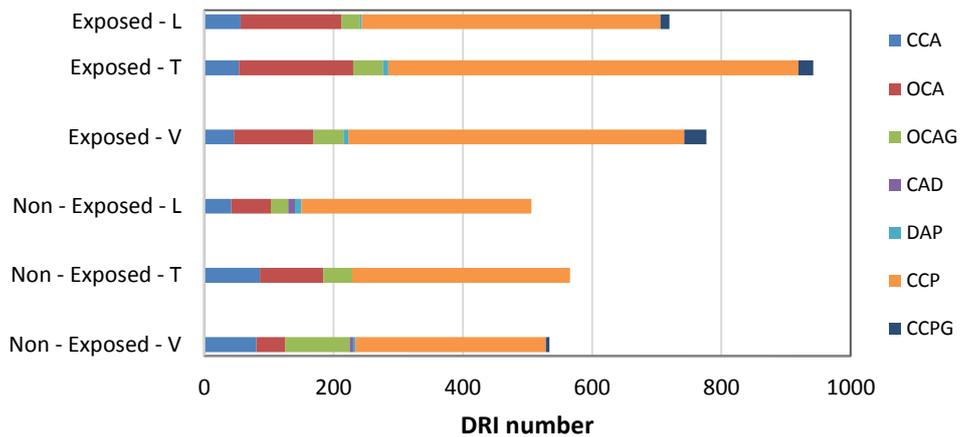

Figure 4.1: Graph illustrating the DRI values for the concrete showing two types of exposure, for three different directions

4.2 Crack pattern

Figure 4.2 illustrates the image analysis conducted through the *ArcGIS* software for both E and NE columns ends.
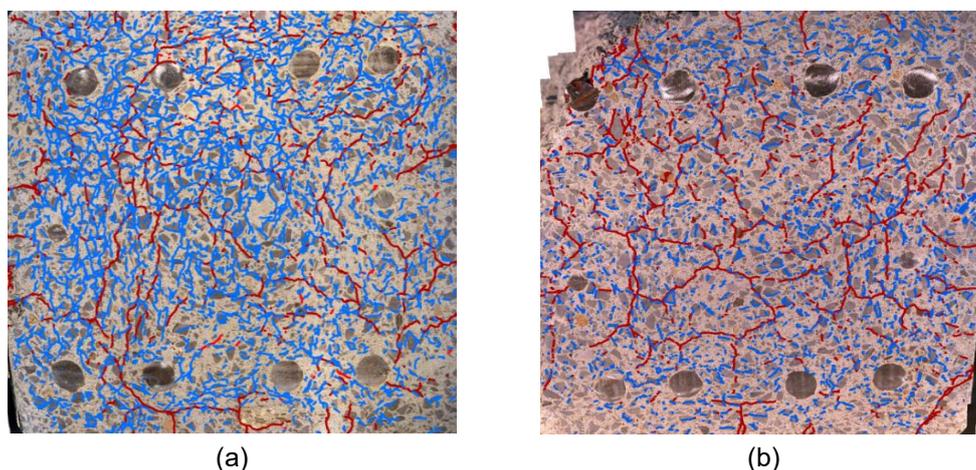

| (a) | (b) |

Figure 4.2: Micro/macroscopic distress features: (a) Exposed column, (b) Non-exposed column.

Evaluating the images above, one verifies that both columns present an important amount of macrocracks (i.e. cracks greater than 0.3 mm - red traces). Moreover, it seems that the macrocracks number is quite comparable for non-exposed and exposed columns. Conversely, the amount of microcracks (i.e. cracks smaller than 0.3 mm – blue traces) is very different from one column to another; the exposed column presents a much higher amount of microcracks when compared to the non-exposed column. Furthermore, and interestingly, the majority of the macrocracks (although not all of them!) seem to be aligned from the top to the bottom of the cross-section of the columns. The latter is in agreement with the stress-state of the columns and DRI results, since the transverse direction presents the least

restrained direction and thus more expansion is expected; therefore a higher amount of open cracks is expected to be developed perpendicularly to this direction.

4.3 Stiffness Damage Test (SDT)

Figure 4.3 presents the average results of two SDT output parameters, as described by Sanchez et al. [4-8]: the *Stiffness Damage Index* (SDI), a measure of the dissipated energy caused by the closure of cracks under compression loads, and the *Plastic Deformation Index* (PDI), which quantifies the slipping across surfaces while the internal cracks close under compression loads. Both indices are a function of the extent of inner cracking present in a given material [4-8]. A full description of the SDI and PDI of the cores can be obtained in [12].

For the non-exposed column, the average SDI values ranged from 0.19 to 0.20, whereas from 0.18 to 0.24 for the exposed ones. Moreover, higher results were obtained in the transverse direction in both columns (direction of less reinforcement).
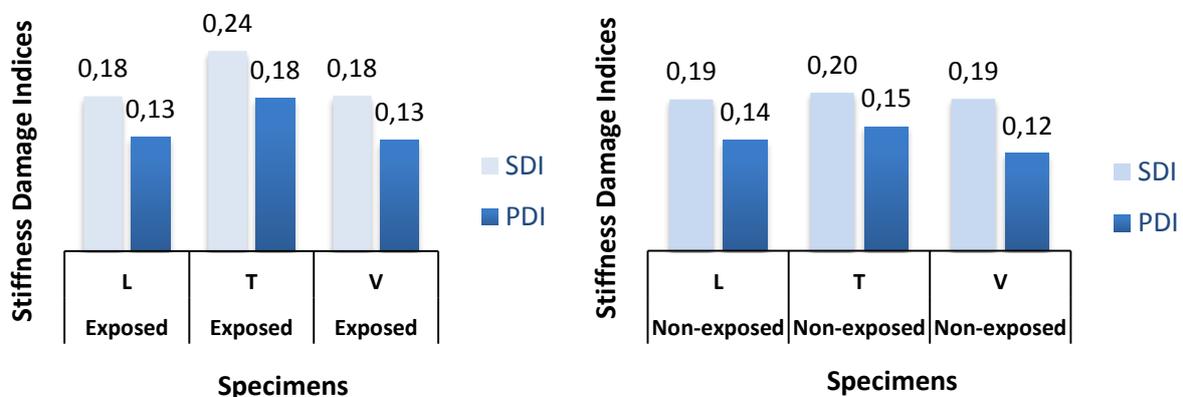

Figure 4.3: SDT indices measured in both non-exposed and exposed columns.

4.4 Stirrups cutting

The stress-relief (µstrains) following the cutting of instrumented stirrups from both columns is presented in Figure 4.4. It is worth mentioning that the columns were stored in the laboratory for several weeks before testing (i.e. no more live loads applied to the structural members); thus, it is fair to consider that the deformations resulting from stress-relief from the stirrups are entirely (or at least largely) related to ASR-induced expansion [12-15].

The stirrups cutting analyses were performed in two ways. First, after cover removal, stirrups were cut at their edges. However, since the stirrups are normally bent at the edges, sometimes attached and close to the columns ends, analyses were also performed in the middle of the column's cross section in order to verify whether higher, and probably more reliable, values could be obtained.

NE column stirrups presented lower deformation values compared to E column stirrups (as expected), especially when the analyses were performed at the middle of the cross section. Actually, comparing data from the edge cuttings (blue bars) and cuttings in the middle of the cross section (red bars), higher values were found in the middle for E column whereas for the edge almost similar values were found for both columns. This suggests that better and more reliable results are obtained from cuttings in the middle section of the stirrups. The average values obtained after cutting in the middle stirrup sections of the non-exposed and exposed columns were respectively 1290 and 570 µstrain.
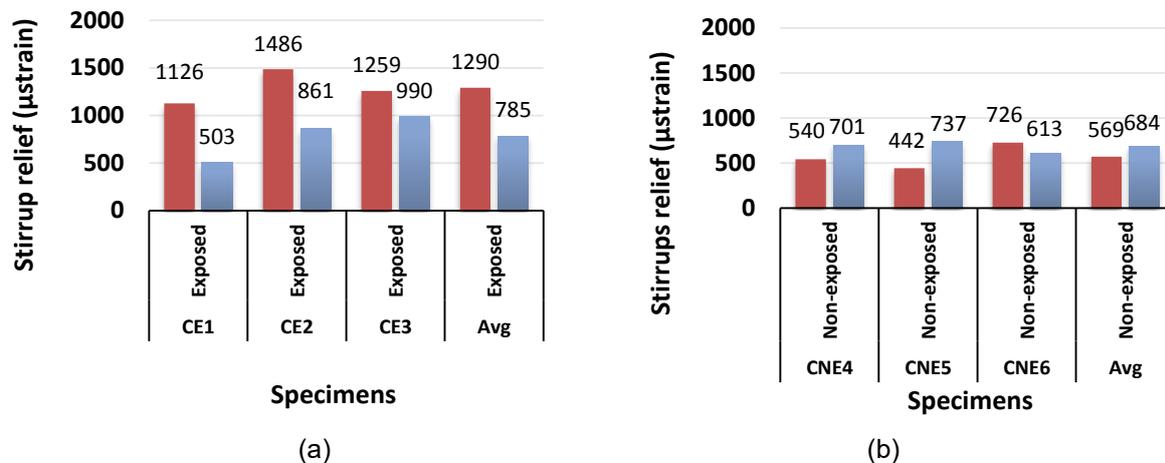
Figure 4.4: Stress-relief measured on the two columns after stirrups cutting: a) Non exposed column; b) Exposed column. Blue bars represent cuts at the stirrups' edges and red bars at the middle of the cross section.

5. DISCUSSION

5.1 Condition assessment of RBC columns

A multi-level approach was proposed by Sanchez et al. [4-8] for the assessment of structures affected by alkali-aggregate reaction (AAR). This approach is based on a combination of microscopic and mechanical tools able to capture the "cause", but especially the "damage extent" of affected concrete. Therefore, the proposed approach enables the diagnosis and indicates future prognosis of ASR-affected concrete. Furthermore, possible structural implications of ASR affected structures and structural components might also be discussed using this procedure.

In this work, the DRI and SDT tests were conducted and the DRI number, SDI and PDI parameters were determined for cores extracted from distinct directions from exposed and non-exposed columns. The DRI values obtained indicate that the amount of damage found for the exposed columns is greater than the non-exposed one. Moreover, distinct values were obtained according to the cores' direction, especially for the E column.

The DRI number of the NE column indicate that the expansion levels reached as per Sanchez et al. [16] were 0,12%, 0,12% and 0,12% for the longitudinal, vertical and transverse directions respectively. Likewise, 0.20%, 0.20% and 0.30% expansion were gathered for the E column samples in the longitudinal, vertical and transverse directions, respectively. Moreover, for both columns, an important number of cracks in the cement paste was observed (CCP) which indicates a severe ASR-induced development at both structural members. Moreover, it is not discarded that some of the measured deterioration in the cement paste might have taken place due to freeze-thaw cycles, which are very common in Canada. Finally, it is important to notice that ASR-gel could only be observed in the cement paste (CCPG) on the exposed columns samples, emphasizing once more the influence of exposure conditions on ASR development, since this feature is associated with high to very high expansion levels (>0.20%).

The image analysis conducted in this work was able to provide a great insight of the crack's propagation inside the column, especially within the reinforcing cage. As it could be observed, both, E and NE demonstrated to have nearly the same amount of macrocracks (i.e. > 0.3% mm). However, the number of microcracks (i.e. < 0.3 mm) are considerably higher in the exposed column. Furthermore, the image analysis highlighted (although only qualitatively for the time being), that the majority of macrocracks seem to be aligned from the top to the bottom of the cross-section of the columns. The latter is in agreement with the microscopic and mechanical results obtained in this work and indicate that further damage is obtained in the direction with the least confinement.

The SDI values obtained in this work were also interesting. For the NE column, very close, if not similar, SDI results were obtained as a function of the cores direction. Moreover, expansion levels of about 0.12% could be attributed to these cores as per Sanchez et al [16]. This result completely matches to the DRI number that did not yield significant differences on the distinct directions of NE samples.

Conversely, the cores extracted from E columns also presented similar average SDI values in the longitudinal and vertical directions (0.18-0.19), yet cores extracted transversely suggested a much higher degree of damage (average SDI of 0.24). The latter confirms the results obtained for the E column on the DRI. The above results are very likely linked to the confinement effects proportioned by the column asymmetric geometry and reinforcement character, which influenced the stress-state and consequently the direction of ASR-induced expansion and damage development. Such results were actually reported by [10] where heterogeneous 3D restraint in structural members were seen to enhance expansion in the direction of the least restraint.

Finally, the results obtained through the stirrups cutting showed that the E column stirrups presented a much higher stress-relief than the NE ones, as expected. Moreover, analysing the data from Figure 4.4, one verifies that the results obtained for the E column seem fairly high, especially because the columns were stored in the laboratory before testing and thus no live loads were still acting on the members when the stirrups were cut. Thus, those values might be directly linked to ASR-induced development and highlight a potential structural concern for stirrups yielding in ASR-affected structures.

6. CONCLUSIONS

The multi-level approach proposed by Sanchez et al. [4-8] was conducted in this work on cores extracted from non-exposed and exposed RBC columns from distinct directions (i.e. longitudinal, vertical and transverse). Moreover, potential yielding of reinforcement (stirrups) in the above elements was evaluated through their stress relief. The main findings of the current research are presented hereafter:

- Different damage degrees are measured according to the coring direction and environmental conditions (i.e. exposed vs non-exposed; longitudinal, vertical and transverse);
- Cores extracted from the exposed column showed more damage than the non-exposed ones, especially those extracted in the transverse direction which is the direction of least restraint in the above columns;
- The Stiffness Damage Test (SDT) and the Damage Rating Index (DRI) are complementary tools for the condition assessment of aging concrete affected by ASR. Both tools indicated the damage degree and were able to differentiate the three coring directions, and also the exposure.
- The environmental conditions have a direct relation with the development of microcracks; however, for macrocracks, the influence was found to be considerably lower (i.e. E and NE presented practically the same amount of macrocracks);
- Concerns may arise regarding yielding of the stirrups in ASR-affected reinforced concrete, especially considering that loading was disregarded in this study. Therefore, the presence of live and service loads could have largely increased the stress state of the stirrups and thus results obtained.

Through the use of DRI and SDI values, along with the damage chart proposed by Sanchez et al [16], it is possible to provide an estimation of the AAR-expansion reached (on average) to date:

- NE column: 0.12% of expansion
- E column: 0.20% of expansion

This above information is critical for the management and structural appraisal of ASR-affected aging infrastructure. Furthermore, it is worth noting that the chart proposed by Sanchez et al [13] may be considered quite conservative, since it has been developed under "free expansion" conditions and thus parameters such as confinement effects, restraints and etc., are not accounted for. Thus, this chart may be treated as the worst-case scenario and should be used carefully while the assessment of reinforced concrete structures in the field.

7. ACKNOWLEDGMENTS

8. REFERENCES

[1] ICAAR Visit Report (2000) Report of the visit of structures affected by AAR in the Quebec City area. 11th International conference on alkali-aggregate reaction, Quebec, Canada

[2] Bérubé MA, Smaoui N, Fournier B, Bissonnette B, Durand B (2005a) Evaluation of the expansion attained to date by concrete affected by ASR - Part III: Application to existing structures. Canadian Journal of Civil Engineering, 32: 463-479.

[3] Bérubé MA, Smaoui N, Bissonnette B, Fournier B (2005b) Outil d'évaluation et de gestion des ouvrages d'art affectés de réactions alcalis-silice (RAS). Studies and research on Transports, Minister of Quebec Transportation, September, 140 p.

[4] Sanchez LFM (2014) Contribution to the assessment of damage in aging concrete infrastructures affected by alkali-aggregate reaction, PhD thesis, Department of Geology and Geological Engineering, Université Laval, Québec, Canada.

[5] Sanchez LFM, Fournier B, Jolin M, Bastien J (2014) Evaluation of the Stiffness Damage Test (SDT) as a tool for assessing damage in concrete due to ASR: test loading and output responses for concretes incorporating fine or coarse reactive aggregates. Cement and Concrete Research, 56: 213-229.

[6] Sanchez LFM, Fournier B, Jolin M, Bastien J (2015a) Evaluation of the Stiffness Damage Test (SDT) as a tool for assessing damage in concrete due to ASR: input parameters and variability of the test responses. Construction and Building Materials, 77: 20-32.

[7] Sanchez LFM, Fournier B, Jolin M, Duchesne J (2015b) Reliable quantification of AAR damage through assessment of the damage rating index (DRI). Cement and Concrete Research, 67: 74-92.

[8] Sanchez LFM, Fournier B, Jolin M, Bastien J, Mitchell D (2015c) Overall damage assessment of concrete distressed due to alkali-silica reaction and freezing and thawing cycles using microscopic and mechanical tools. Construction Materials Conference (CONMAT), August, Whistler, Canada

[9] Inoue S, Mikata Y, Takahashi Y, Inamasu K (2012) Residual shear capacity of ASR damaged reinforced concrete beams with ruptured stirrups. 14th International conference on alkali-aggregate reaction (ICAAR). Texas, USA.

[10] Grattan-Bellew PE, Danay A (1992) Comparison of laboratory and field evaluation of alkali- silica reaction in large dams. International Conference on Concrete Alkali-aggregate Reactions in Hydroelectric Plants and Dams.

[11] Sanchez LFM, Fournier B, Jolin M, Bedoya MAB, Bastien J, Duchesne J (2016) Use of Damage Rating Index to Quantify Alkali-Silica Reaction Damage in Concrete: Fine versus Coarse Aggregate. ACI Materials Journal, 113: 395–407.

[12] Sanchez LFM, Fournier B, Bastien J, Mitchell D, Noel M (2016) Thorough Evaluation Of Bridge Columns Affected By Alkali-silica Reaction (ASR). ICAAR 2016.

[13] Multon S, Toulemonde F (2010) Effect of moisture conditions and transfers on alkali silica reaction damaged structures. Cement and Concrete Research, 40: 924–934.

[14] Fournier B, Bérubé MA (1991) Évaluation du potentiel de réactivité alcaline des granulats à béton produits dans les Basses-Terres du Saint-Laurent du Québec (Canada). Revue canadienne de génie civil, 18(2): 282-296.

[15] Multon S, Dubroca S, Seignol J-F, Toutlemonde F (2004) Flexural Strength of Beams Affected by ASR. 12th ICAAR, Beijing, China.

[16] Sanchez LFM, Fournier B, Jolin M, Mitchell D, Bastien J (2017) Overall assessment of Alkali-Aggregate Reaction (AAR) in concretes presenting different strengths and incorporating a wide range of reactive aggregate types and natures. Cement and Concrete Research, 93: 17-31.